JOURNAL OF



AVIAN BIOLOGY

Research article

Genetic and phenotypic differentiation in *Thamnophilus* ruficapillus, a Neotropical passerine with disjunct distribution in the Andean and Atlantic forests

Belén Bukowski[®] □¹, Leonardo Campagna^{2,3}, Gustavo S. Cabanne¹, Pablo L. Tubaro¹ and Darío A. Lijtmaer¹

Correspondence: Belén Bukowski (belenbukowski@gmail.com)

Journal of Avian Biology 2024: e03293

doi: 10.1111/jav.03293

Subject Editor: Elisa Bonaccorso Editor-in-Chief: Staffan Bensch Accepted 22 July 2024





www.avianbiology.org

The Andean and Atlantic forests are separated by the open vegetation corridor, which acts as a geographic barrier. However, these forests experienced cycles of connection and isolation in the past, which shaped the phylogeographic patterns of their biotas. We analysed the evolutionary history of the rufous-capped antshrike Thamnophilus ruficapillus, a species with a disjunct distribution in the Atlantic and Andean forests and thus an appropriate model to study the effect of the open vegetation corridor and the Andes on the diversification of the Neotropical avifauna. We performed a phylogenetic/phylogeographic analysis, including the five subspecies, using mitochondrial and nuclear genomic DNA, and studied their differences in vocalizations and plumage coloration. Both the mitochondrial and nuclear DNA evidenced a marked phylogeographic structure with three differentiated lineages that diverged without signs of gene flow in the Pleistocene (1.0-1.7 million years ago): one in the Atlantic Forest and two in the Andean forest. However, the two Andean lineages do not coincide with the two disjunct areas of distribution of the species in the Andes. Vocalizations were significantly different between most subspecies, but their pattern of differentiation was discordant with that of the nuclear and mitochondrial DNA. In fact, we did not find song differentiation between the subspecies of the Atlantic Forest and that of the northwestern Bolivian Andes, even though they differ genetically and belong to different lineages. Consistently, no differences were found in plumage coloration between the subspecies of the Atlantic Forest and that of the southern Andes. Our results suggest a complex evolutionary history in this species, which differentiated both due to dispersion across the open vegetation corridor, likely during a period of connection between the Andean and Atlantic forests, and the effect of the Bolivian Altiplano as a geographic barrier. In both cases, Pleistocene climatic oscillations appear to have influenced the species diversification.

Keywords: Andean forest, Atlantic Forest, dispersion, genomic DNA, mitochondrial DNA, phylogenomics, Pleistocene climatic oscillations, plumage coloration, vocalizations

¹División Ornitología, Museo Argentino de Ciencias Naturales 'Bernardino Rivadavia' (MACN-CONICET), Buenos Aires, Argentina

²Fuller Evolutionary Biology Program, Cornell Lab of Ornithology, Ithaca, NY, USA

³Department of Ecology and Evolutionary Biology, Cornell University, Ithaca, NY, USA

^{© 2024} The Author(s). Journal of Avian Biology published by John Wiley & Sons Ltd on behalf of Nordic Society Oikos

This is an open access article under the terms of the Creative Commons Attribution License, which permits use, distribution and reproduction in any medium, provided the original work is properly cited.

Introduction

The main factors that have promoted the diversification of the Neotropical avifauna include the Andes Mountains (Weir 2006, Brumfield and Edwards 2007, Sedano and Burns 2010, Weir and Price 2011), wide rivers (Ribas et al. 2012, Naka and Brumfield 2018, Kopuchian et al. 2020, Thom et al. 2020) and the closure of the Isthmus of Panama (Weir et al. 2009, Smith and Klicka 2010). Although with a more prominent role in the Northern Hemisphere and the southern extreme of South America, the Pleistocene glacial cycles also played a relevant role as avian diversification drivers throughout the Neotropics (Lessa et al. 2003, Weir and Schluter 2004, Lovette 2005, Campagna et al. 2012, Kopuchian et al. 2016, Acosta et al. 2020, Bukowski et al. 2024a). This is clearly the case for highland Andean taxa (Weir 2006, Jetz et al. 2012), but also in the lowlands Pleistocene climatic oscillations may have driven speciation by promoting cycles of contraction, fragmentation and expansion of forest ranges, which generated vicariance, divergence and in some cases secondary contact of both forest and dry habitat species (Rull et al. 2011, Trujillo-Arias et al. 2017, 2020, Silva et al. 2019, Bolívar-Leguizamón et al. 2020, Thom et al. 2020).

Another relevant driver of diversification in the Neotropical region, which until recently has been less studied than those mentioned above, is the open vegetation corridor. This dry strip formed by the Caatinga, Cerrado and Chaco biomes isolates the Amazon and Andean forests from the Atlantic Forest, thus affecting the connectivity of three of the most biodiverse rainforests in the world (Orme et al. 2005). Either by vicariance due to the establishment of the open vegetation corridor in the Neogene in a previously continuous forest or as a consequence of dispersion through these dry habitats after its formation, multiple species of birds are disjunctly codistributed in these forests, with varying degrees of differentiation between forests (Lavinia et al. 2015, 2019, Trujillo-Arias et al. 2017, 2018, 2020, Cabanne et al. 2019, Bocalini et al. 2023).

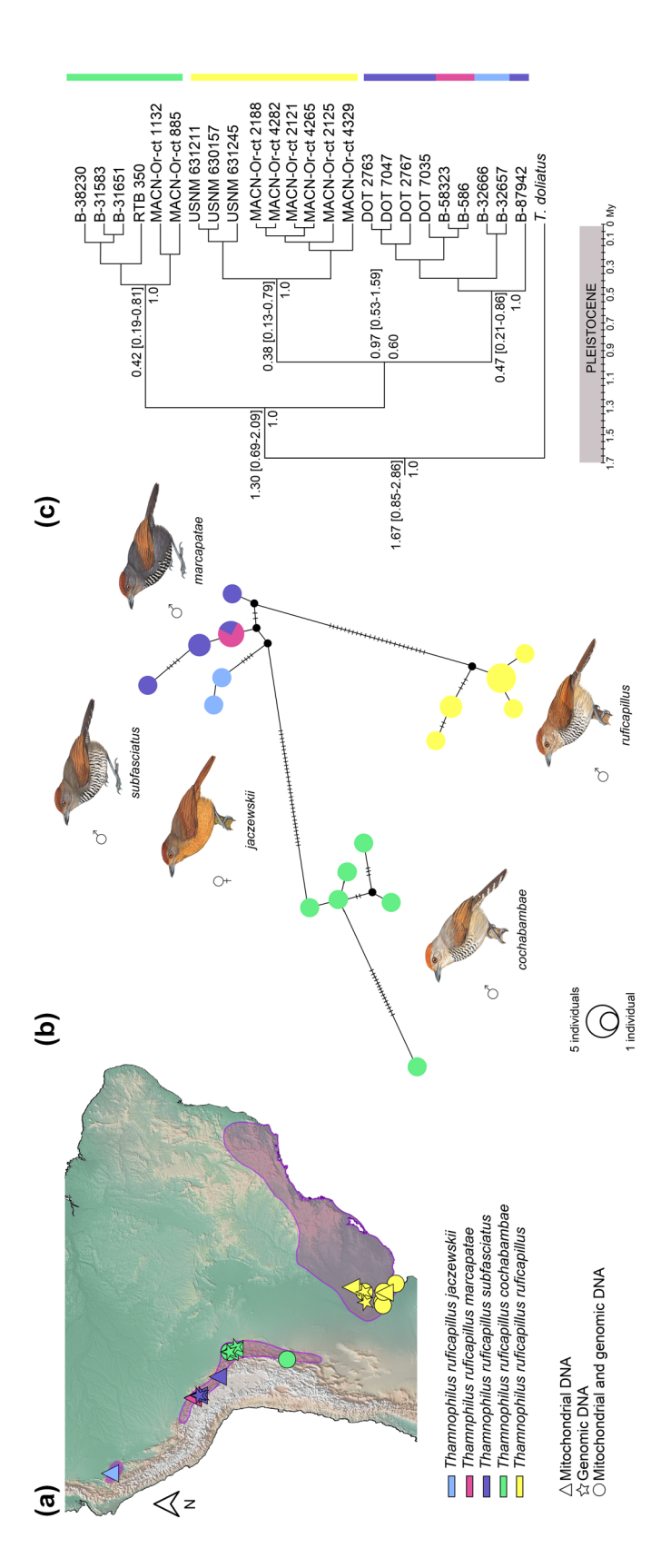
Even though the Andean and Atlantic forests are currently isolated, they have experienced cycles of connection and isolation associated with the geotectonic processes and climatic fluctuations of the Neogene and the Quaternary (Nores 1992, Silva 1994), adding more complexity to this system and its effect on the avifauna of the region (Trujillo-Arias et al. 2017, 2018, 2020, Cabanne et al. 2019, Lavinia et al. 2019). The cyclic connection between these rainforests could have occurred during glacial maxima through the expansions of forests into the Cerrado (Silva 1994), a possibility supported by palynological studies (Ledru 1991, 1993, Oliveira-Filho and Ratter 1995) and avian data (Carnaval and Moritz 2008, Cabanne et al. 2016, 2019, Trujillo-Arias et al. 2017). The contact could have also occurred during interglacial periods through gallery forests in the Chaco region (Olrog 1963, Nores 1992), a hypothesis based mainly on forest bird distribution patterns but without clear evidence (Zurita et al. 2014, Trujillo-Arias et al. 2017). Irrespective of their differences in timing and location, these proposed connections

could have acted in combination (Trujillo-Arias et al. 2017, 2018, 2020).

As shown with other geographic barriers or habitat mosaics in the Neotropics (Smith et al. 2014, Naka and Brumfield 2018, van Els et al. 2021), the effect of this dynamic rainforest history also depends on species-specific ecological characteristics and dispersal abilities (Trujillo-Arias et al. 2018, 2020, Lavinia et al. 2019). Several studies have focused on the evolutionary history of species that inhabit exclusively the Amazon forest or the Atlantic Forest, providing insights into the historical diversification processes operating within these regions (Ribas et al. 2012, Maldonado-Coelho et al. 2013, Cabanne et al. 2016, Silva et al. 2019). Fewer comprehensive evolutionary studies have been performed on species that inhabit both the Atlantic and the Andean or Amazonian forests (Lavinia et al. 2015, 2019, Trujillo-Arias et al. 2017, 2018, 2020, Cabanne et al. 2019, Bolívar-Leguizamón et al. 2020, 2024).

The rufous-capped antshrike *Thamnophilus ruficapillus* has three disjunct areas of distribution, one of them in the Atlantic Forest, and the other two in the Andean forest (Fig. 1a). In the latter, it inhabits humid and semi-humid forests (with different degrees of human alteration) and patches of dense shrubs bordering watercourses in predominantly open areas east of the Andes (Brumfield and Edwards 2007, del Hoyo et al. 2020). In the Atlantic Forest it occurs in low elevation areas of northern Argentina and southern Brazil (Brumfield and Edwards 2007, del Hoyo et al. 2020). Thamnophilus ruficapillus belongs to the group of suboscine passerines, and it is an insectivorous, monogamous and sexually dichromatic species (del Hoyo et al. 2020). Currently, five subspecies are recognized (del Hoyo et al. 2020, Clements et al. 2022): T. r. jaczewskii (in the Andean forest of northern Peru), T. r. marcapatae (in southeastern Peru, particularly Puno and Cusco departments), T. r. subfasciatus (in the Yungas of northwestern Bolivia), T. r. cochabambae (in southern Bolivia to northwestern Argentina) and T. r. ruficapillus (in the Atlantic Forest of southeastern Brazil and northeastern Argentina) (Fig. 1a). Previous analyses of mitochondrial DNA have shown intraspecific divergences of around 4% in the cytochrome c oxidase subunit I (COI) gene between T. r. cochabambae in the Andean forest and T. r. ruficapillus in the Atlantic Forest (Kerr et al. 2009). These estimates are consistent with recent analyses that have shown that the latter is more closely related to T. torquatus (mainly distributed in the Brazilian Cerrado) than to the Andean T. ruficapillus populations (Bolívar-Leguzamón et al. 2024).

Here, we leverage the distribution of *T. ruficapillus* to use this species as a model for the study of the effect of the open vegetation corridor and the Andes on the diversification of the Neotropical avifauna. To achieve this goal, we analysed the evolutionary history of this species using a comprehensive approach that includes both genetic and genomic analyses (mitochondrial and nuclear genomic DNA) as well as phenotypic analyses (study of vocalizations and plumage coloration) to better understand its phylogeographic patterns and the role played by the aforementioned Neotropical diversification drivers.



identity and the type of sequence data obtained for each sample. The distribution map is based on BirdLife International and NatureServe (2014). (b) Median-joining haplotype network of concatenated mDNA (COI + cyt b; 1,130 bp). Circles represent haplotypes and their size is proportional to haplotype frequency. The length of the branches connecting haplotypes is proportional to the number of nucleotide differences between them, which are indicated by the number of line marks on each branch. Colours represent the subspecies phylogenetic tree with divergence times obtained from the analysis of the concatenated mitochondrial dataset (1130 bp). The numbers near the nodes indicate the mean divergence Figure 1. Distribution of T. ruficapillus, sampling information and analyses of mitochondrial DNA. (a) Distribution map (shaded in violet) showing sampling localities, subspecies according to the scheme incorporated in the figure. Black circles represent unsampled hypothetical haplotypes. Bird illustrations by Hilary Burn. © Lynx Nature Books. (c) Bayesian time estimates and the numbers between square brackets correspond to the 95% highest posterior density intervals of those estimates. Divergence times and the numbers between square brackets are in millions of years ago. Posterior probability values are shown below the divergence times. The colours to the right of the tree indicate subspecies information.

Material and methods

Taxon sampling for genetic and genomic analyses

We analysed 29 specimens of T. ruficapillus (24 of which had mitochondrial data and 18 that had nuclear genomic data) from 18 collection sites covering the main distribution range of the species and including representatives of the five subspecies that have been described to date (Fig. 1a, Supporting information). We also included one specimen of T. doliatus and one specimen of T. caerulescens to be used as outgroups (for mitochondrial and genomic phylogenetic reconstructions, respectively). We could not include *T. torquatus*, which has been traditionally considered the sister species of T. ruficapillus (Brumfield and Edwards 2007) but has been very recently suggested to form a species complex with T. ruficapillus (Bolívar-Leguizamón et al. 2024). Subspecies were determined according to the distribution range described by del Hoyo et al. (2020) and Clements et al. (2022), and we specifically checked that the localities in which each specimen had been captured were not ambiguous in relation to the subspecies inhabiting that area. Moreover, and in the case of Andean subspecies that are in close proximity, the samples used were collected either in or very close to the type locality for each subspecies.

Laboratory protocols for mitochondrial markers

We extracted DNA from fresh tissue (pectoral muscle or blood) following the silica-based protocol described by Ivanova et al. (2006), using individual spin columns (Lijtmaer et al. 2012). We amplified two mitochondrial genes: cytochrome c oxidase I (COI) and cytochrome *b* (cyt *b*). Primers used for the amplification of the 695 base pairs (bp) of the COI were BirdF1 (Hebert et al. 2004) and COIbirdR2 (Kerr et al. 2009) and to amplify 1007 bp of the cyt *b* we used L14841 (Kocher et al. 1989) and H16065 (Lougheed et al. 2000).

PCR amplification reaction cocktails and the thermocycling profile for COI from fresh tissue followed Lijtmaer et al. (2012). To amplify the cyt *b* we followed the protocol in Arrieta et al. (2013) and the PCR cocktail was prepared in a 20 μl volume with the following reagents: 3 μl of genomic DNA, 1x PCR buffer, 0.2 mM dNTPs, 3 mM Cl₂Mg/SO₄Mg, 0.5 μM of each primer (forward and reverse) and 1U Taq DNA polymerase (Invitrogen). The PCR thermocycling profile was as follows: 3 min at 94°C; 40 cycles of 45 s at 94°C, 30 s at 53°C and 1 min at 72°C; and finally 10 min at 72°C.

Sequencing of both mitochondrial markers was conducted at Macrogen Korea (Seoul, Korea) and performed bidirectionally with the same primers used for amplification. GenBank accession numbers for all sequences generated in this study are included in the Supporting information.

Laboratory protocols for nuclear genomic markers

We extracted genomic DNA from fresh tissue samples using DNeasy tissue extraction kit (Qiagen). To generate the genomic data we used double-digest restriction site-associated

DNA sequencing (ddRADseq) following the protocol of Peterson et al. (2012) with modifications described in Thrasher et al. (2018). Briefly, for each sample we isolated ~ 500 ng of DNA, at a standardized concentration of 20 ng/µl, and digested it with the restriction enzymes SbfI High Fidelity (8 base bp recognition site; 5'-CCTGCAGG-3') and MspI (4 base bp recognition site; 5'-CCGG-3') (New England BioLabs). The digested DNA was ligated to P1 and P2 adapters on both ends (sequences are available in Peterson et al. 2012). We size-selected groups of 20 uniquely barcoded samples (index groups), retaining fragments between 400 and 700 bp using Blue Pippin (Sage Science). To incorporate the full Illumina TruSeq primer sequences and unique indexing primers into each library, we performed low cycle number PCR with Phusion High-Fidelity DNA Polymerase (New England BioLabs), with the following thermocycling profile: 98°C for 30 s followed by 11 cycles at 98°C for 5 s, 60°C for 25 s, and 72°C for 10 s with a final extension at 72°C for 5 min. We visualized the product of this amplification on a 1% agarose gel and performed a final 0.73 AMPure cleanup to eliminate DNA fragments smaller than 200 bp. Finally, sequencing was performed on an Illumina HiSeq 2500 lane at the Cornell University Biotechnology Resource Center as part of a larger sequencing batch, obtaining single-end 150bp sequences, with an average mean sequencing depth of 151 reads per locus per individual (range: 104-220).

Genetic diversity and population structure based on mitochondrial markers

To perform the mitochondrial genetic analyses, we edited and aligned COI and cyt *b* sequences using CodonCode Aligner ver. 4.0.4 (CodonCode Corporation) and carefully checked the chromatograms for ambiguities and the aligned sequences to detect the presence of any stop codons, as well as alignment gaps.

Because mitochondrial sequences are linked within the same genome, COI and cyt b sequences were concatenated for the analyses. First, to analyse the genetic variation within the species and understand the relationship among haplotypes, we calculated the average p distances using MEGA7 (Kumar et al. 2016) and generated haplotype networks using the median joining algorithm implemented in PopART ver. 1.0 (http://popart.otago.ac.nz), respectively. We conducted an analysis of molecular variance (AMOVA) in Arlequin ver. 3.5 (Excoffier and Lischer 2010) to explore the distribution of genetic variation within T. ruficapillus and specifically test whether there are differences in the frequency of mitochondrial haplotypes among subspecies. The Φ_{ST} values between pairs of subspecies were computed using uncorrected genetic distance matrices between haplotypes and significance was tested through 2000 random permutations.

Phylogenetic analyses and divergence time estimations based on mitochondrial DNA

We inferred gene trees with Bayesian, maximum parsimony (MP) and maximum likelihood (ML) methodologies using

MrBayes ver. 3.2.2 (Ronquist et al. 2012), TNT ver. 1.1 (Goloboff et al. 2003) and MEGA7, respectively. The bestfit model of nucleotide substitution for each locus for the Bayesian analysis was selected using the Bayesian information criterion (BIC) implemented in jModelTest ver. 2.1.1 (Darriba et al. 2012). HKY+I was chosen for COI and KHY for cyt b (Hasegawa et al. 1985). Both loci were placed in unlinked partitions allowing parameters to vary and to be estimated independently (except for topology and branch lengths). We conducted two independent runs of 10 million generations sampling trees every 100 generations under default priors for all parameters. We discarded the first 25% of the sampled trees as burn-in and the remaining 75 000 trees of each run were combined to generate a majority rule consensus tree. The standard deviation of split frequencies (SDSF) between runs was always < 0.01, indicating convergence. Using Tracer ver. 1.7 (Rambaut et al. 2018), we checked that both runs reached the stationary phase and that we had a good sample of the posterior probability distributions. For the MP analysis we ran heuristic searches based on 1000 random addition sequences (RAS) coupled with the tree bisection reconnection (TBR) branch-swapping algorithm, saving 10 trees per replication. A strict consensus tree was estimated from the collection of most parsimonious trees. To estimate node support we conducted a bootstrap analysis (Felsenstein 1985) that consisted of 1000 pseudoreplicates of 100 RAS+TBR saving 10 trees per replicate. The ML analysis was based on the Kimura 2-parameter model (Kimura 1980) with a bootstrap of 500 replicates. The initial trees for the heuristic search were obtained automatically by applying the maximum parsimony method. The tree with the highest likelihood was chosen.

The time of the mitochondrial divergence between T. ruficapillus and T. doliatus, as well as the time of the separation of the mitochondrial lineages within T. ruficapillus, were estimated by generating a time-calibrated ultrametric tree with the Bayesian approach implemented in BEAST ver. 1.8 (Drummond et al. 2012). Both mitochondrial markers were placed in separate partitions with unlinked substitution and clock models selected with jModelTest: HKY+I for COI and HKY for cyt b. The tree models were linked since the mitochondria is a single unit of inheritance. We specified a Yule speciation tree prior, assuming a constant population size and a relaxed uncorrelated lognormal clock. We used a calibration of 2.1% per million years (My) for cyt b (1.05 × 10⁻² substitutions/site/lineage/My; Weir and Schluter 2008) and 1.17×10^{-2} substitutions/site/lineage/My for COI (Lavinia et al. 2016). We conducted two independent runs of 100 million generations sampling trees every 1000 generations. We used Tracer to explore the combined traces and checked for stationarity in the estimation of the parameters and adequate ESS values. We combined the two independent runs with LogCombiner ver. 1.8 (Drummond et al. 2012). Finally, we discarded the first 10% of the sampled trees (burn-in = 10 000), summarized the node heights as the median node heights and then estimated the 95% highest posterior density (HPD) intervals of divergence dates using TreeAnnotator ver. 1.8 (Drummond et al. 2012).

Population structure and phylogenetic analysis based on genomic DNA

We demultiplexed, trimmed, filtered reads, assembled loci and called single nucleotide polymorphism (SNPs) with Ipyrad ver. 0.7.28 (Eaton and Overcast 2020). We discarded sequences when a single base had a Phred quality score below 10 or more than 5% of bases had a Phred quality score below 20. Additional filtering was applied to only retain reads that did not have enzyme cleavage sites, adaptor sequences or index sequences. We used the default settings within Ipyrad to assemble loci and call SNPs: cluster threshold was set to 0.85, maximum fraction of heterozygous bases allowed in consensus sequences was set to 0.05, maximum number of SNPs allowed in a final locus was set to 0.2, maximum number of ambiguous sites was set to 0.05 and maximum number of shared polymorphic sites in a locus was set to 0.5. Finally, we only kept loci that were present in at least 80% of the samples. The ddRAD data is available in Dryad (https://doi. org/10.5061/dryad.tb2rbp09k).

We performed a principal component analysis (PCA), using the 'gdsfmt' and 'SNPRelate' packages (Zheng et al. 2012) in R ver. 3.5.1 (www.r-project.org), to visualize possible clusters in the data. We used all the SNPs of the dataset (including multiple SNPs per locus), but because the PCA is sensitive to missing data, SNPs missing from at least one individual were removed, resulting in 2306 SNPs for this analysis. We also assigned individuals to genetic clusters (K) using Structure ver. 2.3.4 (Pritchard et al. 2000). For this analysis we used a single random SNP from each RAD locus, resulting in 5,073 SNPs. We implemented the admixture ancestry model with correlated allele frequencies and an allele frequency prior of $\lambda = 1$. We conducted 10 runs for each value of K = 1-4, and each run consisted in 500 000 generations following a burnin of 100 000. The most likely value of K was determined following the ΔK method described by Evanno et al. (2005) and implemented in Structure Harvester ver. 0.6.94 (Earl and vonHoldt 2012). We averaged results across the 10 runs using the greedy algorithm in the program CLUMPP ver. 1.1.2 (Jakobsson and Rosenberg 2007) and visualized results using the 'conStruct' package (Bradburd et al. 2018) in R.

We used RAxML ver. 8.2.4 (Stamatakis 2014) to infer a maximum likelihood phylogenetic tree starting from the dataset of 14 724 SNPs (all SNPs in each locus), and subsequently retaining the 10 591 SNPs for which the minor allele was in homozygosity in at least one individual. We implemented the ASC_GTRGAMMA model and the Lewis correction for ascertainment bias, and we conducted 200 bootstrap replicates to assess node support. We included one specimen of *T. caerulescens* as outgroup for this analysis and thus re-assembled loci following the same parameters described above (we obtained ddRADseq data for this specimen from a previous study; Kopuchian et al. 2020; Supporting information).

Demographic history modeling

We used the Generalized Phylogenetic Coalescent Sampler (G-PhoCS) ver. 1.2.3 (Gronau et al. 2011) to estimate divergence times, effective population sizes and gene flow. We used unphased sequence data without filtering for minor allele frequency to avoid biasing our demographic model. The dataset consisted of 6165 RADseq loci containing 13 485 SNPs. Because of the computationally intensive nature of this analysis, we restricted our data set to a maximum of 10 individuals per subspecies, selecting one individual per location. We ran G-PhoCS using the standard MCMC settings described in Gronau et al. (2011) and default parameters with 75 000 burn-in generations and 750 000 additional sampling generations. We assessed adequate mixing and convergence using Tracer. Divergence times and effective population sizes were converted from mutation scale to generations (T) and individuals (Ne) respectively, by assuming an average mutation rate of 10⁻⁹ mutations per bp per generation (Kumar and Subramanian 2002). The model implemented in G-PhoCS is conditioned upon a given phylogenetic topology. Thus, we ran G-PhoCS using the topology of the nuclear genomic tree (which is concordant with the Bayesian, MP and ML mitochondrial trees).

Song analyses

We analysed 50 recordings belonging to the five subspecies of *T. ruficapillus* and covering the entire geographic distribution range of the species (Supporting information). Recordings were in 'wav' format and were obtained from the Macaulay Library of Natural Sounds (Cornell Lab of Ornithology) and Xeno-Canto (http://www.xeno-canto.org).

We generated and analysed the spectrograms using Raven Pro ver. 1.5 (www.birds.cornell.edu/raven). The conditions for the analyses were a 512 fast Fourier transform length with a 50% overlap, a Hamming window type, and a grayscale colour scheme. We analysed one song per individual choosing the one with the best signal-to-noise ratio. Songs in this species consist of a repetition of similar notes. The first note is the longest, followed by successively shorter notes, until the last note, which is longer and similar to the first one. We measured three variables in the first harmonic (which has the higher amplitude): mean duration of the note, mean duration of the interval between notes and bandwidth of the note (difference between the maximum and minimum frequencies of the note). In addition, we counted the number of notes in each song and measured the fundamental frequency (calculated as the difference in frequency between the note with the lowest frequency and the first harmonic, and measured in the centre of each harmonic; Supporting information). Variables were measured on the first note, then additionally averaged between the second, fourth and sixth note to obtain a measurement of the intermediate notes, and finally again on the last note.

To assess vocal variation we performed a PCA in R and analysed the data with a one-way analysis of variance (ANOVA; all the principal component scores met the

assumptions of homoscedasticity and normality). We then performed Bonferroni contrasts to assess differences among subspecies in their PC scores using SPSS ver. 15.0.1(SPSS Inc.). All variables were standardized (i.e. scaled so that each of them had a mean of 0 and a standard deviation of 1) previous to the analysis and we considered that variables were significantly correlated with a PC only when the module of their factor loading value was greater than 0.7 (Tabachnick and Fidell 2001).

Finally, we also performed an ANOVA using the original song variables, followed by Bonferroni contrasts, because this can provide a more detailed analysis of specific differences among subspecies.

Plumage colouration analyses

To objectively describe plumage colour variation within *T. ruficapillus*, we obtained reflectance spectra measurements from museum skins deposited at the MACN (Supporting information). We measured five males and four females of *T. r. cochabambae* and 30 males and 18 females of *T. r. ruficapillus*, which are the only two subspecies present in Argentina and available in the MACN collection. We used only adult specimens that were in excellent preservation condition for reflectance measurements.

Male plumage in this species is mostly brown (T. r. cochabambae and T. r. ruficapillus) or dark gray (T. r. jaczewskii, T. r. marcapatae and T. r. subfasciatus), with rufous wings, a rufous or chestnut cap and barred underparts and tail. The species is sexually dichromatic, with brown females in all subspecies (i.e. no grey plumage) and either lack or very faint barring in their underparts and no white marking in their tales (Supporting information). Taking into account this colour patterning, we measured reflectance in six plumage patches on each specimen: throat, breast, belly, crown, nape and back. All reflectance measurements were performed with an Ocean Optics USB 2000 spectrometer (Ocean Optics Inc.) with a PX-2 pulsed xenon light source (effective range of emission from 220 to 750 nm), calibrated against a WS-1 diffuse reflectance white standard (Ocean Optics Inc.). Plumage was illuminated and reflectance data were collected with a bifurcated probe housed in a prismatic holder that was held against the chosen region on the study skin. The probe was held with an angle of 90° to the surface of the plumage patch. The diameter of the circular measured area was approximately 6 mm, and the distance between the probe and the plumage was 23 mm.

We performed analyses using the 'pavo' package in R (Maia et al. 2013). Because this species is sexually dichromatic, males and females were analysed separately. We evaluated colour differentiation in the chromatic component between subspecies for each plumage patch by estimating a perceptual distance (ΔS) using the Vorobyev and Osorio (1998) colour discrimination model. Colour perceptual distances are expressed in terms of just noticeable differences (jnd) and a value of 1.0 jnd represents the theoretical threshold for discrimination of two colours, meaning that it is the

Table 1. Genetic pairwise comparisons among the five subspecies of *Thamnophilus ruficapillus* based on mitochondrial DNA (COI+cyt b). Above the diagonal: pairwise $\Phi_{s\tau}$ values; significant values (p < 0.05) in bold. Diagonal: mean uncorrected genetic distances within each subspecies. Below the diagonal: mean uncorrected genetic distances between pairs of subspecies. Genetic distances are expressed in percentage values.

Subspecies	T. r. jaczewskii	T. r. marcapatae	T. r. subfasciatus	T. r. cochabambae	T. r. ruficapillus
T. r. jaczewskii	0.1	0.92	0.59	0.83	0.73
T. r. marcapatae	0.6	0	0.15	0.82	0.70
T. r. subfasciatus	0.8	0.2	0.4	0.83	0.73
T. r. cochabambae	3.5	3.3	3.4	0.7	0.74
T. r. ruficapillus	3	2.6	2.7	3.6	0.3

distance in the perceptual colour space at which two colours would be visually discernible (Barreira et al. 2021). Thus, $\Delta S > 1.0$ jnd indicates significant colour discrimination by the birds in all light conditions (Vorobyev et al. 1998, Siddiqi et al. 2004). In addition, we determined the statistical significance of the estimated ΔS values for each plumage patch comparison between subspecies (Maia and White 2018). For this, we estimated the geometric average of ΔS values for all comparisons performed between subspecies and calculated the 95% confidence interval (CI) through a bootstrap analysis with the bootcoldist function of pavo in R. We also tested the significance of these comparisons through a PERMANOVA analysis with the adonis function of the 'vegan' package in R (Oksanen et al. 2008).

Results

Genetic diversity and population structure based on mitochondrial markers

We analysed the concatenated mitochondrial DNA sequences (COI + cyt b = 1,130 bp) of 24 individuals of *T. ruficapillus* belonging to the five subspecies (Supporting information). The specimens were collected in 16 localities from Peru, Bolivia, Argentina and Uruguay, covering a wide range of the species distribution (Fig. 1a). Our results showed considerable variation within T. ruficapillus and, in particular, the subspecies that inhabits the Atlantic Forest, T. r. ruficapillus, clearly differed from the four Andean subspecies, with a mean genetic distance between 2.6% and 3.6% (p-distance; Table 1). There was also considerable variation among the Andean subspecies, with T. r. cochabambae showing the highest genetic divergence both with respect to T. r. ruficapillus and with the remaining Andean subspecies (Table 1). Lower levels of genetic distance were observed between T. r. subfasciatus, T. r. marcapatae and T. r. jaczewskii and in fact we found almost no genetic divergence (0.2%) between T. r. subfasciatus and T. r. marcapatae.

Both the haplotype network (Fig. 1b) and the AMOVA (Table 1) show a marked phylogeographic structure within *T. ruficapillus*, with three clearly differentiated lineages: one formed by the subspecies present in the Atlantic Forest (*T. ruficapillus*), another by the subspecies distributed in the Andes of southern Bolivia and northwestern Argentina (*T. r. cochabambae*), and the last one containing the remaining Andean subspecies from northern Bolivia to Peru (Fig. 1b).

Phylogenetic analyses and diversification dating based on mitochondrial DNA

Bayesian, maximum parsimony (MP) and maximum likelihood (ML) reconstructions recovered T. ruficapillus as monophyletic in relation to *T. doliatus* with maximum statistical support (Supporting information). The time-calibrated ultrametric phylogeny (Fig. 1c) shows that the split between them occurred 1.67 million years ago (Mya) (95% HDP: 0.85-2.86). These reconstructions show three clades that correspond to the lineages described above: one includes the subspecies from the Atlantic Forest (T. r. ruficapillus), another one is formed by T. r. cochabambae and the third one by T. r. subfasciatus, T. r. jaczewskii and T. r. marcapatae (Fig. 1c, Supporting information). In the case of the Bayesian, MP and ML reconstructions the oldest split was between the subspecies from the Atlantic Forest and those from the Andean forest (Supporting information), with low values of both posterior probability and bootstrap support between the two Andean clades (0.63, 63% and 64%, respectively). However, the time-calibrated ultrametric phylogeny indicated that the first split within the species, which occurred in the Pleistocene approximately 1.30 Mya (95% HPD: 0.69-2.09 Mya), was between the southernmost Andean subspecies (T. r. cochabambae) and the rest of the subspecies (Fig. 1c). This analysis suggested a more recent divergence between the subspecies from the Atlantic Forest (T. r. ruficapillus) and the clade that includes the rest of the Andean subspecies (T. r. subfasciatus, T. r. jaczewskii and T. r. marcapatae), approximately 0.97 Mya (95% HPD: 0.53-1.59 Mya). This split, however, also had low support (posterior probability: 0.60; Fig. 1c).

Population structure, phylogenetic tree and demographic history modelling based on ddRAD markers

We obtained reduced-representation genomic data for 18 specimens of *T. ruficapillus* collected in 11 localities from

Bolivia, Argentina and Uruguay that belong to the subspecies *T. r. ruficapillus*, *T. r. cochabambae* and *T. r. subfasciatus* (Fig. 1a, Supporting information) and represent the three clades obtained with mitochondrial DNA. The de novo assembly produced a total of 6165 RADseq loci (13 485 SNPs) present in at least 80% of the individuals. This data set was used to perform the analyses described below with the exception of the maximum likelihood reconstruction analysis, in which we included an outgroup and thus re-assembled loci (final dataset 14 724 SNPs).

Nuclear genomic variation was congruent with the results described for mitochondrial DNA, showing a clear differentiation between the three lineages. First, individuals clustered in the PCA in three clearly differentiated groups which corresponded to each of the subspecies (Fig. 2a). The Structure analysis also supported the three main groups, as K=3 had the highest ΔK value and the highest mean log likelihood (Supporting information), and the three genomic clusters correspond to the mitochondrial lineages (Fig. 2b). Only one individual of *T. r. ruficapillus* from Uruguay presented mixed genomic content, but the proportion of its genome assigned to the *subfasciatus* cluster was very low (less than 5%). The rest of the individuals did not show admixture in their genome. These results suggest that gene flow among these three subspecies is either absent or very low.

The maximum likelihood reconstruction recovered a topology with three clades that match the clusters obtained in the Structure and PCA analyses, which also coincide with the mitochondrial lineages (Fig. 2c). All nodes had maximum bootstrap support. The first split within the species occurred between *T. r. ruficapillus* (from the Atlantic Forest) and the subspecies from the Andean forest (*T. r. cochabambae* and *T. r. subfasciatus*), with a subsequent separation between these Andean subspecies. This topology is congruent with those obtained in the MP, Bayesian and ML analyses with mitochondrial data (but differ from the topology of the calibrated ultrametric tree; Fig. 1c, Supporting information).

Our demographic analysis in G-PhoCS was based on the topology of the nuclear phylogeny, which indicated that the initial split occurred between the eastern T. r. ruficapillus and the Andean subspecies (T. r. cochabambae and T. r. subfasciatus), with a subsequent separation between the latter. The result, however, indicated that the three lineages split almost at the same time (Fig. 3): T. r. ruficapillus diverged from the other two subspecies 1.693 million generations ago (Mga) (95% confidence interval: 1.482-1.968 Mga) and the two Andean subspecies diverged from each other only 440 generations after this first split (1.692 Mga, 95% confidence interval: 1.482-1.967). The effective population size of each of the subspecies is between one third and half of the ancestral effective population size estimated for the species (~ 1.5 M individuals). However, the most noticeable result in this regard is the very small estimated ancestral effective population size of the lineage leading to T. r. subfasciatus and T. r. cochabambae, which was estimated to be only 313 individuals. This result suggests that this population could have experienced a bottleneck after (or during) its split from T. r.

ruficapillus, expanding afterwards to reach the current effective population size of the Andean subspecies (~ 0.4 M and ~ 0.55 M individuals; Fig. 3). This is consistent with the fact that Andean populations could have been isolated in refugia during the glacial periods after their split from T. r. ruficapillus (Chaves et al. 2011). Finally, this analysis also confirmed that there has been very low gene flow between subspecies (Fig. 3), a result consistent with the PCA and Structure analyses. All estimations of migration between lineages are orders of magnitude below 1, suggesting that their diversification has occurred in isolation.

Vocalization analyses

The PCA shows differences in vocalizations among subspecies. The first three PCs explained 65% of song variation. PC1 correlated with the fundamental frequency of the first and the last note, PC2 correlated with the mean duration of the first and intermediate notes and PC3 did not strongly correlate with any song variable (Supporting information). Subspecies statistically differed in PC1 (F=11.32, p < 0.01) and PC2 (F=18.43, p < 0.01), whereas no significant differences were found for PC3 (F=2.87, p=0.09). In particular, pairwise comparisons showed that T. r. jaczewskii significantly differed from T. r. ruficapillus and T. r. cochabambae in PC1 and from T. r. marcapatae in PC2 (Supporting information). In turn, T. r. cochabambae differed from all subspecies in PC2 (Supporting information). These differences can be observed in the space delimited by the first two PCs (Fig. 4). No differences were found in the rest of the pairwise comparisons between subspecies for PC1, PC2 or PC3 (Supporting information).

The results of the individual song variables provided more detail about song variation and showed substantial differentiation among subspecies. In fact, the ANOVA indicated significant differences for most song variables (Supporting information). Moreover, the Bonferroni contrasts showed significant differences in at least one variable for almost all subspecific comparisons, with the only exceptions of T. r. subfasciatus vs. T. r. ruficapillus and T. r. subfasciatus vs. T. r. marcapatae (Supporting information). Therefore, and consistently with the PCA result, both T. r. jaczewskii and T. r. cochabambae significantly differed in their songs from all other subspecies, being the subspecies with the most differentiated vocalizations. In addition. T. r. jaczewskii was the subspecies that differed in more song variables from the rest (and particularly so from T. r. cochabambae and T. r. ruficapillus) (Supporting information).

Colouration analyses

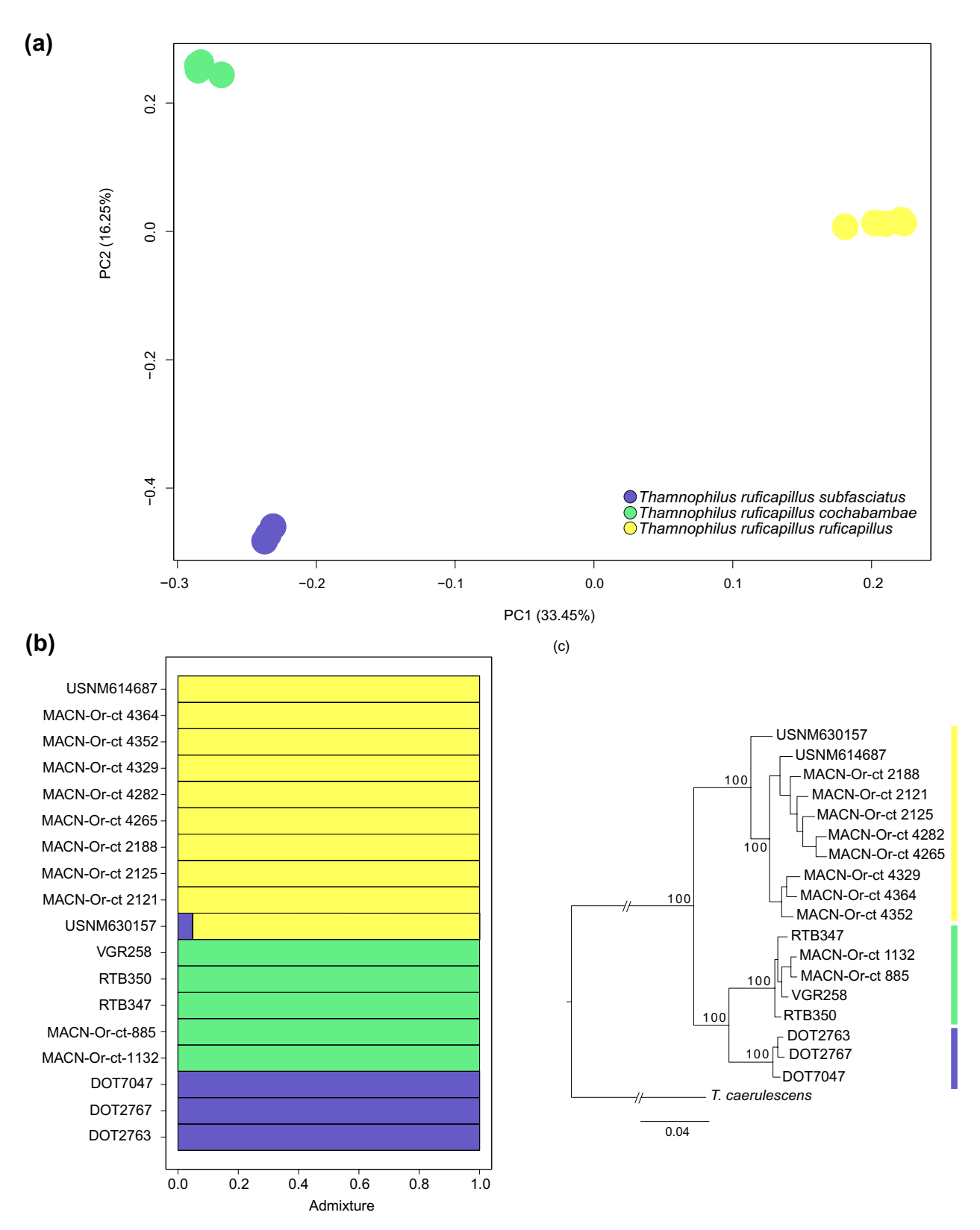


Figure 2. Genomic analyses of *T. ruficapillus*. (a) Principal component analysis (PCA) based on 2306 SNPs (SNPs present in all individuals). (b) Structure plot for K=3 based on 5073 SNPs (one random SNP per RAD locus). (c) Phylogeny inferred with maximum likelihood; the colours to the right of each individual indicate the subspecies. The tree was rooted with *Thamnophilus caerulescens*. Bootstrap support values are indicated in the nodes.

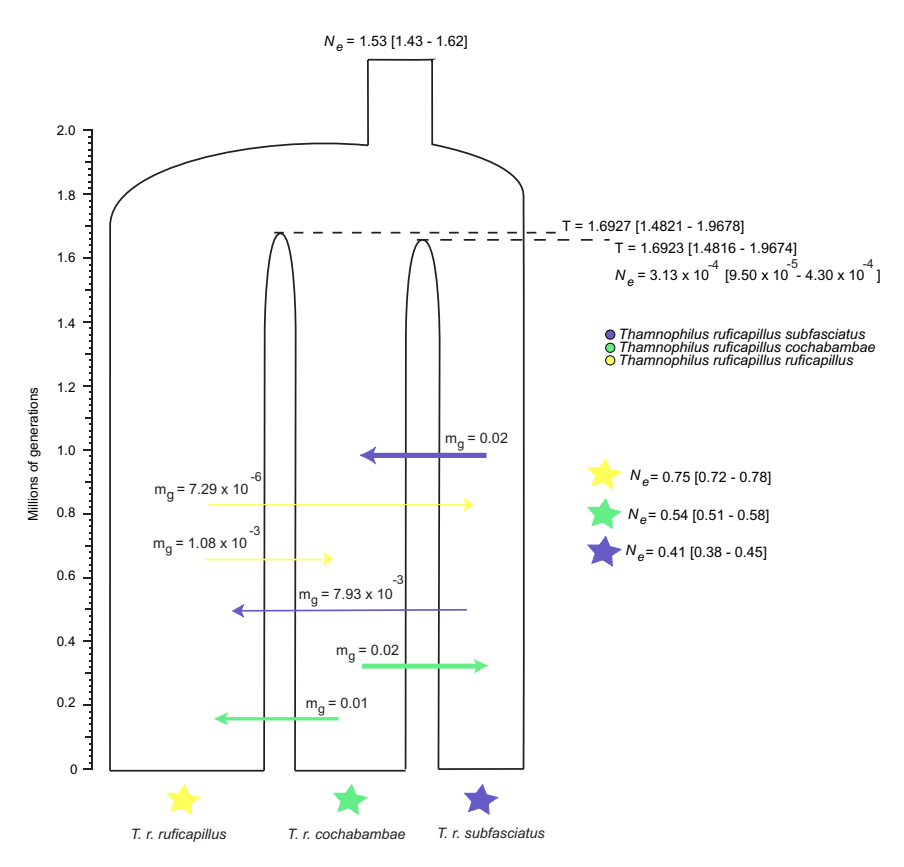


Figure 3. Demographic reconstruction of *T. ruficapillus* based on 6165 RADseq loci (13 485 SNPs). Estimates of divergence times (T; in millions of generations), migration rates (mg; in migrants per generation) and current and ancestral effective population sizes (Ne; in millions of individuals) are reported with their 95% confidence intervals.

same two subspecies showed differences higher than 1.00 jnd for three plumage patches: throat, belly and nape (Table 2). The PERMANOVA, however, was not significant for any of the comparisons (Table 2), suggesting that the variation between subspecies was not significantly higher than the variation within each of them neither for females nor for males. This relatively subtle, non-significant colour differentiation between subspecies can also be observed in the reflectance spectra of the patches (Supporting information).

Discussion

The combination of mitochondrial and nuclear DNA, complemented with data on vocalizations and plumage coloration, allowed us to study the evolutionary history of *T. ruficapillus*. Our findings provide a good starting point towards understanding the history of diversification of this species, the relative patterns of genotypic and phenotypic variation, and the role played by the open vegetation corridor and the Andes Mountains in this process.

First, the mitochondrial DNA results suggest that the split between *T. doliatus* and the lineage that includes *T. ruficapillus* and *T. torquatus* occurred 1.67 Mya, within the Pleistocene. These two taxa were very recently shown to constitute a species complex (Bolívar-Leguizamón et al.

2024), and their internal diversification therefore took place even more recently than the split with *T. doliatus*. In particular, the diversification within *T. ruficapillus* generated a

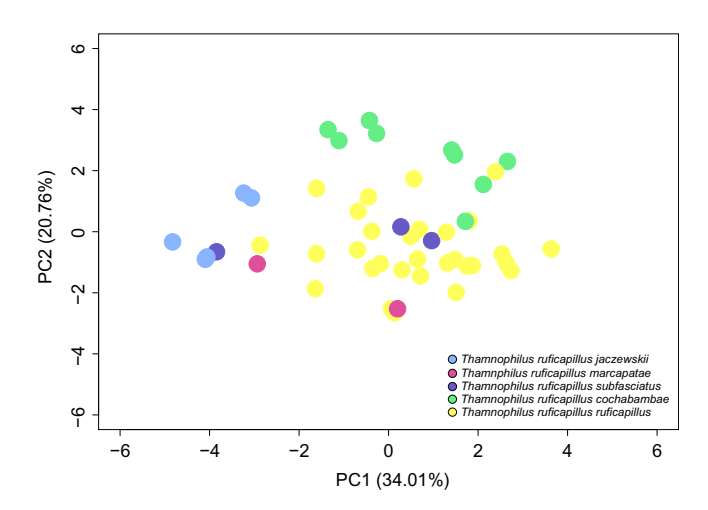


Figure 4. Analysis of the vocalizations of *T. ruficapillus*. Song differentiation among subspecies is shown based on a PCA performed with the song variables (mean duration of the note, mean duration of the interval between notes, fundamental frequency, bandwidth of the note and the number of notes in each song; the first four variables were measured for the first note).

Table 2. Colour differentiation (ΔS) among females of *T. r. ruficapillus* and *T. r. cochabambae*, and among males of *T. r. ruficapillus* and *T. r. cochabambae*. ΔS represents relative chromatic perceptual distance between females of the two subspecies analyzed and between males of the two subspecies analyzed for each plumage patch. Values are geometric means (and 95% confidence intervals) for all comparisons. The unit of ΔS is jnd (just noticeable differences). Values above 1.0 jnd, the theoretical threshold for colour discrimination, are underlined. The PERMANOVA results were statistically not significant in all comparisons.

Plumage patch	Females			Males		
	N T. r. ruficapillus	N T. r. cochabambae	ΔS	N T. r. ruficapillus	N T. r. cochabambae	ΔS
Throat	18	4	1.39 (0.22-3.24)	30	5	1.12 (0.39-2.32)
Breast	18	4	1.63 (0.48-2.77)	30	5	0.91 (0.24-1.89)
Belly	18	4	1.53 (0.54-2.59)	30	5	1.61 (0.67-2.57)
Crown	18	4	2.31 (0.59-4.45)	30	5	0.71 (0.41-2.61)
Nape	18	4	2.34 (0.89-3.75)	30	5	1.20 (0.42-6.95)
Back	18	4	0.99 (0.24–2.72)	30	5	0.46 (0.24–1.99)

phylogeographic structure with three main genetic lineages: one in the Atlantic Forest (T. r. ruficapillus), another one including the southernmost Andean subspecies (T. r. cochabambae), and finally one lineage formed by the three remaining Andean subspecies (T. r. subfasciatus, T. r. marcapatae and T. r. jaczewskii). The various analyses based on both the mitochondrial DNA and the nuclear genome recovered these three genetic clusters (although we note that for genomic analyses we were only able to include T. r. subfasciatus as a representative of the northern Andean lineage). If we consider that T. torquatus has been recently shown to constitute another lineage within the T. ruficapillus/T. torquatus species complex (Bolívar-Leguizamón et al. 2024), we can state that this species complex includes four lineages, two in the Andean forest, one in the Atlantic Forest and one that includes the northern Atlantic Forest and the Cerrado.

The relationship between the three *T. ruficapillus* main lineages is not clear and it can actually be considered a polytomy. The Bayesian, MP and ML mitochondrial reconstructions, as well as the nuclear genomic phylogeny, suggested that the first split within T. ruficapillus took place between the lineage from the Atlantic Forest and an Andean lineage, with a subsequent separation within the latter. However, the time-calibrated ultrametric phylogeny based on mitochondrial data inferred that the first split occurred between the two Andean lineages. Surprisingly, the topology of this ultrametric phylogeny indicates that shortly after the Andean split, the colonization of the lowland areas of the Atlantic Forest occurred from the northern Andean lineage and not from the lineage that inhabits northwestern Argentina and southern Bolivia, which is geographically much closer to the Atlantic Forest. This discordance in the relationship among linages could be due to the temporal proximity of both splits, a result common to all analyses. In particular, the time-calibrated ultrametric phylogeny based on mitochondrial DNA suggested that the first split within T. ruficapillus (in this reconstruction the split between the two Andean lineages) occurred approximately 1.3 Mya, and the colonization of the Atlantic Forest approximately 1 Mya. The G-PhoCS analysis, which was based on nuclear DNA, suggested that the two splits between lineages took place approximately 1.7 million generations ago. If we consider that the generation time for passerines could be estimated to be around 1 year on average (Wang 2004, Cabanne et al. 2008), these two results (from the analyses of mitochondrial and nuclear genomic DNA) are relatively concordant and are also consistent with the results reported by Bolívar-Leguizamón et al. (2024) that included *T. torquatus*.

Consistent with the temporal proximity of these two deepest splits within T. ruficapillus and their different sequence of occurrence depending on the reconstruction methodology, one should note that the support of the nodes that define the relationship of these three lineages was very low in all mitochondrial reconstructions (63% and 64% bootstrap support in the MP and ML analyses, 0.63 posterior probability in the Bayesian phylogeny and 0.60 posterior probability in the time-calibrated phylogeny; Fig. 1c, Supporting information). In addition to the temporal proximity between these two splits, there could be incomplete lineage sorting due to the recency of this diversification, which could also be at least in part responsible for the differences in the topologies of the phylogenetic reconstructions. Regardless of the subtle difference in the timing of the splits and the uncertainty in their order, our results are congruent in suggesting that the main events of diversification of T. ruficapillus that generated its current patterns of population diversity emerged in a short time period during the Pleistocene, shortly after the origin of the species (and the same is true when considering the entire T. ruficapillus/ T. torquatus species complex).

Taking together our genetic and genomic results, including the virtual absence of gene flow between the Atlantic Forest and Andean forest populations, we can confirm the role of the open vegetation corridor as a geographic barrier for T. ruficapillus. Nevertheless, the origin of the allopatric populations of this species should be explained as a result of dispersal through the open vegetation corridor and not as a vicariance event due to its establishment. This is because the Atlantic Forest and the Andean forest became isolated by this barrier before the Pleistocene (Costa 2003, Trujillo-Arias et al. 2017, Cabanne et al. 2019, Lavinia et al. 2019, Bolívar-Leguizamón et al. 2024) and therefore before the origin of T. ruficapillus and the split between its Atlantic and Andean lineages (which is dated to approximately 1-1.7 Mya by our analyses). This suggests a relevant role of the Pleistocene climatic cycles on the diversification of *T. ruficapillus*, since the dispersion through the open vegetation corridor could have occurred during one of the periods of connection between the Atlantic and Andean forests. If the first split within the species occurred between the eastern and western lineages (as

suggested by most of our analyses, including the phylogeny based on genomic DNA), it is difficult to establish the direction of the dispersion and colonization. On the other hand, if the first split occurred within the Andes (as suggested by the time-calibrated Bayesian analysis), it could be considered that the species originated in the mountain range and dispersed to the east after its first split between the Andean lineages. In this second scenario, the Bayesian phylogeny indicates that the colonization occurred from the northern lineage of the Andean forest, suggesting that it could have taken place across the Cerrado as proposed by Silva (1994), and not across the Chaco as hypothesized by Nores (1992). This route across the Cerrado is consistent with the presence of the fourth lineage of this species complex in the Brazilian Cerrado (*T. torquatus*) and the fact that the Atlantic Forest populations of T. ruficapillus have been recently shown to be actually more closely related to *T. torquatus* than to the Andean populations of *T.* ruficapillus (Bolívar-Leguizamón et al. 2024). In conclusion, even though we can assume the dispersal through the open vegetation corridor and a relevant role of Pleistocene climatic cycles in this process, it is clear that the diversification of T. ruficapillusl T. torquatus has been complex and that it is not simple to establish the sequence of splits that occurred. Moreover, the fact that *T. doliatus*, the sister species of the *T.* ruficapillus/ T. torquatus complex, is widely distributed in the Neotropics, precludes us from assuming which is the area in which the split that originated this species complex occurred and thus establishing the subsequent order of diversification events. Further studies with a more geographically comprehensive sampling of *T. ruficapillus* and the inclusion of *T. torquatus* and *T. doliatus* are needed to fully elucidate this matter.

The Andes Mountains have also played a relevant role in the diversification of *T. ruficapillus*, as indicated by the existence of two distinct Andean lineages with remarkably low gene flow. Surprisingly, these two lineages do not coincide with the two disjunct areas of distribution of this species in the Andes, at least from a mitochondrial perspective (Fig. 1). One of these lineages is formed by the populations of T. r. cochabambae from northwestern Argentina and southern Bolivia. The other lineage is constituted by the three remaining Andean subspecies from northern Bolivia and Peru, T. r. subfasciatus, T. r. marcapatae and T. r. jaczewskii. These subspecies span both areas of disjunct distribution in the mountain range and only exhibit low mitochondrial sequence divergence in the case of T. r. jaczewskii, the northern subspecies that is geographically isolated. This pattern suggests that the Bolivian Altiplano seems to be a geographic barrier separating both Andean lineages, which in fact coincides with phylogeographic breaks found in the same area in various other montane bird species (Cadena et al. 2007, Álvarez-Varas et al. 2015, Gutiérrez-Pinto et al. 2019). Given that our analyses indicated that the divergence between these two Andean lineages occurred around 1.3-1.7 Mya, during the Pleistocene, one could hypothesize that Pleistocene climatic oscillations have also played a role in the diversification of this species in the Andes (Weir 2006, 2009, Chaves et al. 2011, Valderrama et al. 2014).

The vocal analyses showed significant differences in one or various song variables between most of the subspecies, which at first glance seems to be consistent with the presence of a marked phylogeographic structure. In fact, only two of the subspecies comparisons did not show vocal differentiation. One of them was between T. r. subfasciatus and T. r. marcapatae, which were also the pair of subspecies with the lowest genetic divergence and shared haplotypes. The second pair of subspecies without song differences was T. r. ruficapillus and T. r. subfasciatus, an unexpected result given that they belong to different mitochondrial lineages and their areas of distribution are disjunct, with the former present in the Atlantic Forest and the latter in the Andean forest of northwestern Bolivia. On the other extreme of our results, T. r. jaczewskii was one of the most vocally differentiated subspecies, significantly differing in its song from all other subspecies. This result could be expected given that T. r. jaczewskii is geographically isolated from the other populations of the species, but contrasts with the relatively shallow mitochondrial DNA differentiation in this subspecies (nuclear DNA could not be analysed), particularly when compared with T. r. subfasciatus and T. r. marcapatae, which in fact are part of its same mitochondrial lineage but significantly differed in their songs.

The finding of these discordances between the genetic/ genomic patterns of divergence and vocal differentiation in T. ruficapillus is surprising given that this species is a suboscine, and therefore its song is likely developed without learning (Kroodsma and Konishi 1991, Isler et al. 1998, Touchton et al. 2014), being free from the influence of cultural evolution and possessing a more direct connection with genetic divergence than in oscines (Seddon 2005). In fact, previous intraspecific studies of suboscine song variation have shown more concordant patterns of vocal and genetic structuring (Isler et al. 2005, Acero-Murcia et al. 2021, Bukowski et al. 2024b). However, some studies have shown cases of divergent lineages lacking song differentiation in suboscines (García et al. 2018) and other birds with innate songs (Nwankwo et al. 2017), as was the case for T. r. ruficapillus and T. r. subfasciatus in this study. Future vocal studies of this species should analyse the putative effect of natural and sexual selection, which could cause different patterns of song variation compared to neutral genetic markers even in species with innate songs (García et al. 2018, 2023). On the other hand, the vocal pattern of variation in this species can also be affected by the adaptation to habitat characteristics and their effect on sound transmission. This could delay or accelerate song differentiation in relation to genetic phylogeographic patterns, depending on the similarity or disparity of the various forest types along the species distribution (Morton 1975, Wiley 1991, Seddon 2005, Tubaro and Lijtmaer 2006).

Finally, and in spite of their allopatry and marked mitochondrial and nuclear DNA differentiation, no significant differences were found between the Atlantic Forest subspecies *T. r. ruficapillus* and the Andean subspecies *T. r. cochabambae* in plumage coloration (neither for males nor for females). The lack of correlation between colour differentiation and genetic divergence among intraspecific lineages has been found in

previous studies of Neotropical birds (Trujillo-Arias et al. 2020, Paulo et al. 2023), but analyses including the remaining three subspecies, as well as a larger geographic sampling, are needed to better assess the pattern of colour variation in this species.

Final remarks

Our analyses of the evolutionary history of T. ruficapillus shows that the T. ruficapillus/T. torquatus species complex originated in the Late Pleistocene, within the last 1.7 million years, and diversified into four clearly differentiated lineages: one lineage in the Atlantic Forest, one lineage in the northern Atlantic Forest and the Cerrado and two different lineages in the Andes, with a split in western Bolivia. This pattern of genetic variation highlights the relevance of the open vegetation corridor and likely the Bolivian Altiplano as diversification drivers for *T. ruficapillus*, likely in combination with the effect of the Pleistocene climatic cycles. Levels of phenotypic variation, however, are partially discordant with this genetic structuring. Songs are significantly differentiated among subspecies, but their geographic pattern of variation does not coincide with that shown by mitochondrial or nuclear DNA. We found clearly differentiated songs between subspecies that are genetically similar and, on the contrary, lack of detectable song differentiation between the Atlantic Forest subspecies and that of northwestern Bolivia in the Andes, which present a substantial genetic differentiation and belong to different lineages. Similarly, plumage colouration between the Atlantic Forest subspecies and that of the southern Andes did not differ significantly. Future studies should address these discordances with an increased sampling and the analysis of the effect of evolutionary and ecological pressures on song and colour. Finally, our results are in accordance with those of other birds with disjunct populations in the Atlantic and Andean forests for which the open vegetation corridor has promoted diversification (Lavinia et al. 2015, 2019, Trujillo Arias et al. 2018, 2020, Cabanne et al. 2019). However, these studies show that the level of differentiation between the populations of these forests is notoriously heterogeneous, suggesting an idiosyncratic effect of this barrier and the cycles of connection and isolation of these forests and highlighting the importance of comparative analyses to better understand the role of the main drivers of avian Neotropical diversification and speciation.

Acknowledgements — We thank the collectors and staff of the institutions that loaned tissue samples used in this study: American Museum of Natural History; Burke Museum, Smithsonian Institution, National Museum of Natural History and Louisiana State University Museum of Natural Science. We also thank the Macaulay Library of Natural Sounds and the recordists who deposited their *Thamnophilus* recordings in Xeno-Canto. We also thank the fauna offices of Buenos Aires and Jujuy provinces, the National Ministry of Environment and Sustainable Development of Argentina, and the National Parks Administration of Argentina for granting the permits needed for this study. We specially thank

Yolanda Davies and Laura Barone from the Museo Argentino de Ciencias Naturales "Bernardino Rivadavia" for their assistance with various logistic aspects of this study, including specimen curation and tissue sampling. We thank Bronwyn Butcher from the Fuller Evolutionary Biology Lab (Cornell Lab of Ornithology) for help generating the genomic data.

Funding – This study was funded by the Consejo Nacional de Investigaciones Científicas y Tecnológicas (CONICET) from Argentina, the Agencia Nacional de Promoción de la Investigación, el Desarrollo Tecnológico y la Innovación from Argentina, the Richard Lounsbery Fundation and Fundación Williams.

Permits – Below are the numbers of the relevant permits used to collect tissue samples for this study granted by the Offices of Fauna of Jujuy and Buenos Aires provinces (PCJU20051, PCBA20071 and GT10014), and Parque Nacional El Palmar (PCPN20081) in Entre Ríos province. The details of the museum skins used in this study are provided in the Supporting information.

Author contributions

Belén Bukowski: Conceptualization (equal); Data curation (lead); Formal analysis (lead); Methodology (lead); Writing - original draft (lead); Writing - review and editing (equal). Leonardo Campagna: Conceptualization (equal); Data curation (supporting); Formal analysis (supporting); Methodology (supporting); Resources (supporting); Software (supporting); Supervision (supporting); Writing – review and editing (equal). Gustavo S. Cabanne: Conceptualization (equal); Data curation (supporting); Formal analysis (supporting); Methodology (supporting); Software (supporting); Writing – review and editing (equal). Pablo L. Tubaro: Conceptualization (equal); Formal analysis (supporting); Funding acquisition (lead); Methodology (supporting); Resources (lead); Supervision (supporting); Writing – review and editing (equal). Darío A. Lijtmaer: Conceptualization (equal); Formal analysis (supporting); Funding acquisition (lead); Methodology (lead); Project administration (lead); Resources (lead); Supervision (lead); Writing – original draft (lead); Writing – review and editing (equal).

Data availability statement

Data are available from the Dryad Digital Repository: https://doi.org/10.5061/dryad.tb2rbp09k (Bukowski et al. 2024b).

Supporting information

The Supporting information associated with this article is available with the online version. DOI of four COI sequences can be found in Table S1.

References

Acero-Murcia, A. C., Raposo do Amaral, F., de Barros, F. C., da Silva Ribeiro, T., Miyaki, C. Y. and Maldonado-Coelho, M. 2021. Ecological and evolutionary drivers of geographic variation in songs of a Neotropical suboscine bird: the drab-breasted bamboo tyrant (*Hemitriccus diops*, Rhynchocyclidae). – Ornithology 138: 1–15.

- Acosta, I., Cabanne, G. S., Noll, D., González-Acuña, D., Pliscoff,
 P. and Vianna, J. A. 2020. Patagonian glacial effects on the endemic green-backed firecrown, *Sephanoides sephaniodes* (Aves: Trochilidae): evidence from species distribution models and molecular data. J. Ornithol. 162: 289–301.
- Álvarez-Varas, R., González-Acuña, D. and Vianna, J. A. 2015. Comparative phylogeography of co-distributed *Phrygilus* species (Aves, Thraupidae) from the Central Andes. – Mol. Phylogenet. Evol. 90: 150–163.
- Arrieta, R. S., Lijtmaer, D. A. and Tubaro, P. L. 2013. Evolution of postzygotic reproductive isolation in galliform birds: analysis of first and second hybrid generations and backcrosses. – Biol. J. Linn. Soc. 110: 528–542.
- Barreira, A. S., Eaton, M. D., Vilacoba, E., Tubaro, P. L. and Kopuchian, C. 2021. Shortwavelength visual sensitivity and sexual differences in plumaje colouration of ovenbirds (Aves: Furnarinae). J. Ornithol. 162: 737–748.
- Bocalini, F., Bolívar-Leguizamón, S. D., Silveira, L. F. and Bravo, G. A. 2023. Amazonian colonization from the Atlantic Forest: new perspectives on the connections of South American tropical forests. – Mol. Ecol. 32: 6874–6895.
- Bolívar-Leguizamón, S. D., Bocalini, F., Silveira, L. F. and Bravo, G. A. 2024. The role of biogeographical barriers on the historical dynamics of passerine birds with a circum-Amazonian distribution. Ecol. Evol. 14: e10860.
- Bolívar-Leguizamón, S. D., Silveira, L. F., Derryberry, E. P., Brumfield, R. T. and Bravo, G. A. 2020. Phylogeography of the variable antshrike (*Thamnophilus caerulescens*), a South American passerine distributed along multiple environmental gradients. Mol. Phylogenet. Evol. 148: 106810.
- Bradburd, G. S., Coop, G. M. and Ralph, P. L. 2018. Inferring continuous and discrete population genetic structure across apace. Genetics 210: 33–52.
- Brumfield, R. T. and Edwards, S. V. 2007. Evolution into and out of the Andes: a bayesian analysis of historical diversification in *Thamnophilus* antshrikes. Evolution 61: 346–367.
- Bukowski, B., Campagna, L., Rodríguez-Cajarville, M. J., Cabanne, G. S., Tubaro, P. L. and Lijtmaer, D. A. 2024a. The role of glaciations in the evolutionary history of a widely distributed Neotropical open habitat bird. J. Biogeogr. 51: 199–214.
- Bukowski, B., Campagna, L., Cabanne, G. S., Tubaro, P. L. and Lijtmaer, D. A. 2024b. Data from: Genetic and phenotypic differentiation in a Neotropical passerine with a disjunct distribution in the Andean and Atlantic forests (*Thamnophilus ruficapillus*). – Dryad Digital Repository, https://doi.org/10.5061/ dryad.tb2rbp09k.
- Cadena, C. D., Klicka, J. and Ricklefs, R. E. 2007. Evolutionary differentiation in the Neotropical montane region: molecular phylogenetics and phylogeography of *Buarremon brushfinches* (Aves, Emberizidae). – Mol. Phylogenet. Evol. 44: 993–1016.
- Cabanne, G. S., d'Horta, F. M., Sari, E. H. R., Santos, F. R. and Miyaki, C. Y. 2008. Nuclear and mitochondrial phylogeography of the Atlantic forest endemic *Xiphorhynchus fuscus* (Aves: Dendrocolaptidae): biogeography and systematics implications. Mol. Phylogenet. Evol. 49: 760–773.
- Cabanne, G. S., Calderón, L., Trujillo Arias, N., Flores, P., Pessoa, R., d'Horta, F. M. and Miyaki, C. Y. 2016. Pleistocene climatic changes affected species ranges and evolutionary processes in the Atlantic Forest. Biol. J. Linn. Soc. 119: 856–872.
- Cabanne, G. S., Campagna, L., Trujillo-Arias, N., Naoki, K., Gómez, I., Miyaki, C. Y., Santos, F. R., Dantas, G. P. M., Aleixo, A., Claramunt, S., Rocha, A., Caparroz, R., Lovette, I. J. and Tubaro, P. L. 2019. Phylogeographic variation within the

- Buff-browed foliage-gleaner (Aves: Furnariidae: *Syndactyla rufo-superciliata*) supports an Andean-Atlantic forests connection via the Cerrado. Mol. Phylogenet. Evol. 133: 198–213.
- Campagna, L., St Clair, J. J. H., Lougheed, S. C., Woods, R. W., Imberti, S. and Tubaro, P. L. 2012. Divergence between passerine populations from the Malvinas – Falkland Islands and their continental counterparts: a comparative phylogeographical study. – Biol. J. Linn. Soc. 106: 865–879.
- Carnaval, A. C. and Moritz, C. 2008. Historical climate modelling predicts patterns of current biodiversity in the Brazilian Atlantic forest. J. Biogeogr. 35: 1187–1201.
- Chaves, J. A., Weir, J. T. and Smith, T. B. 2011. Diversification in *Adelomyia* hummingbirds follows Andean uplift. Mol. Ecol. 20: 4564–4576.
- Clements, J. F., Schulenberg, T. S., Iliff, M. J., Fredericks, T. A., Gerbracht, J. A., Lepage, D., Billerman, S. M., Sullivan, B. L. and Wood, C. L. 2022. The eBird/Clements checklist of Birds of the World: v2022. https://www.birds.cornell.edu/clementschecklist/download/.
- Costa, L. P. 2003. The historical bridge between the Amazon and the Atlantic Forest of Brazil: a study of molecular phylogeography with small mammals. J. Biogeogr. 30: 71–86.
- Darriba, D., Taboada, G. L., Doallo, R. and Posada, D. 2012. JModelTest 2: more models, new heuristics and parallel computing. – Nat. Methods 9: 772.
- del Hoyo, J., Zimmer, K., Collar, N., Isler, M. L. and Kirwan, G. M. 2020. Rufous-capped antshrike (*Thamnophilus ruficapillus*), ver. 1.0. In: Billerman, S. M., Keeney, B. K., Rodewald, P. G. and Schulenberg, T. S., (eds), Birds of the World. Cornell Laboratory of Ornithology.
- Drummond, A. J., Suchard, M. A., Xie, D. and Rambaut, A. 2012. Bayesian phylogenetics with BEAUti and the BEAST 1.7. Mol. Biol. Evol. 29: 1969–1973.
- Earl, D. A. and vonHoldt, B. M. 2012. Structure Harvester: a website and program for visualizing Structure output and implementing the Evanno method. – Conserv. Genet. Resour. 4: 359–361.
- Eaton, D. A. R. and Overcast, I. 2020. ipyrad: interactive assembly and analysis of RADseq data sets. Bioinformatics 36: 2592–2594.
- Evanno, G., Regnaut, S. and Goudet, J. 2005. Detecting the number of clusters of individuals using the software Structure: a simulation study. Mol. Ecol. 14: 2611–2620.
- Excoffier, L. and Lischer, H. E. L. 2010. Arlequin suite ver. 3.5: A new series of programs to perform population genetics analyses under linux and windows. Mol. Ecol. Resour. 10: 564–567.
- Felsenstein, J. 1985. Confidence limits on phylogenies: an approach using the bootstrap. Evolution 39: 783–791.
- García, N. C., Campagna, L., Rush, A. C., Bowie, R. C. K. and Lovette, I. J. 2023. Comparative genomics of two *Empidonax* flycatchers reveal candidate genes for bird song production. – Evolution 77: 1818–1828.
- García, N. C., Naka, L. N. and Cabanne, G. S. 2018. Vocal variation in relation to genetic structure in an Atlantic forest woodcreeper (*Xiphorhynchus fuscus*): evolutionary and taxonomic implications. J. Ornithol. 159: 379–388.
- Goloboff, P., Farris, J. and Nixon, K. 2003. T.N.T.: tree analysis using new technology. Program and documentation. http://www.zmuc.dk/public/phylogeny.
- Gronau, I., Hubisz, M. J., Gulko, B., Danko, C. G. and Siepel, A. 2011. Bayesian inference of ancient human demography from individual genome sequences. Nat. Genet. 43: 1031–1034.
- Gutiérrez-Pinto, N., McCracken, K. G., Tubaro, P. L., Kopuchian, C., Astie, A. and Cadena, C. D. 2019. Molecular,

- niche, and morphological differentiation among torrent duck (*Merganetta armata*) populations in the Andes. Zool. Scr. 48: 589–604.
- Hasegawa, M., Kishino, K. and Yano, T. 1985. Dating the humanape splitting by a molecular clock of mitochondrial DNA. J. Mol. Evol. 22: 160–174.
- Hebert, P. D. N., Stoeckle, M. Y., Zemlak, T. S. and Francis, C. M. 2004. Identification of birds through DNA barcodes. – PLoS Biol. 2: e312.
- Isler, M. L., Isler, P. R. and Brumfield, R. T. 2005. Clinal variation in vocalizations of an antibrid (*Thamnophilidae*) and implications for defining species limits. – Auk 122: 433–444.
- Isler, M. L., Isler, P. R. and Whitney, B. M. 1998. Use of vocalizations to establish species limits in antibrds (Passeriformes: *Thamnophilidae*). Auk 115: 577–590.
- Ivanova, N. V., deWaard, J. R. and Hebert, P. D. N. 2006. An inexpensive, utomation-friendly protocol for recovering highquality DNA. – Mol. Ecol. Notes 6: 998–1002.
- Jakobsson, M. and Rosenberg, N. A. 2007. Clumpp: a cluster matching and permutation program for dealing with label switching and multimodality in analysis of population structure. – Bioinformatics 23: 1801–1806.
- Jetz, W., Thomas, G. H., Joy, J. B., Hartmann, K. and Mooers, A. O. 2012. The global diversity of birds in space and time. – Nature 491: 444–448.
- Kerr, K. C. R., Lijtmaer, D. A., Barreira, A. S., Hebert, P. D. N. and Tubaro, P. L. 2009. Probing evolutionary patterns in Neotropical birds through DNA barcodes. PLoS One 4: e4379.
- Kocher, T. D., Thomas, W. K., Meyer, A., Edwards, S. V., Pääbo, S., Villablanca, F. X. and Wilson, A. C. 1989. Dynamics of mitochondrial DNA evolution in animals: amplification and sequencing with conserved primers. Proc. Natl Acad. Sci. USA 86: 6196–6200.
- Kopuchian, C., Campagna, L., Di Giacomo, A. S., Wilson, R. E.,
 Bulgarella, M., Petracci, P., Mazar Barnett, J., Matus, R., Blank,
 O. and McCracken, K. G. 2016. Demographic history inferred
 from genome-wide data reveals two lineages of sheldgeese
 endemic to a glacial refugium in the southern Atlantic. J.
 Biogeogr. 43: 1979–1989.
- Kopuchian, C., Campagna, L., Lijtmaer, D. A., Cabanne, G. S., García, N. C., Lavinia, P. D., Tubaro, P. L., Lovette, I. and Di Giacomo, A. S. 2020. A test of the riverine barrier hypothesis in the largest subtropical river basin in the Neotropics. – Mol. Ecol. 29: 2137–2149.
- Kroodsma, D. E. and Konishi, M. 1991. A suboscine bird (eastern phoebe, *Sayornis phoebe*) develops normal song without auditory feedback. Anim. Behav. 42: 477–487.
- Kumar, S. and Subramanian, S. 2002. Mutation rates in mammalian genomes. Proc. Natl Acad. Sci. USA 99: 803–808.
- Kumar, S., Stecher, G. and Tamura, K. 2016. MEGA7: molecular evolutionary genetics analysis ver. 7.0 for bigger datasets. – Mol. Biol. Evol. 33: 1870–1874.
- Lavinia, P. D., Barreira, A. S., Campagna, L., Tubaro, P. L. and Lijtmaer, D. A. 2019. Contrasting evolutionary histories in Neotropical birds: divergence across an environmental barrier in South America. – Mol. Ecol. 28: 1730–1747.
- Lavinia, P. D., Escalante, P., García, N. C., Barreira, A. S., Trujillo-Arias, N., Tubaro, P. L., Naoki, K., Miyaki, C. Y., Santos, F. R. and Lijtmaer, D. A. 2015. Continental-scale analysis reveals deep diversification within the polytypic red-crowned ant tanager (*Habia rubica*, Cardinalidae). Mol. Phylogenet. Evol. 89: 182–193.
- Lavinia, P. D., Kerr, K. C. R., Tubaro, P. L., Hebert, P. D. N. and Lijtmaer, D. A. 2016. Calibrating the molecular clock beyond

- cytochrome b: assessing the evolutionary rate of COI in birds. J. Avian Biol. 47: 84–91.
- Ledru, M. P. 1991. Etude de la pluie pollinique actuelle des forêts du Brésil Central: climat, végétation, application à l'étude de l'évolution paléoclimatique des 30 000 dernières années. – Quaternaire 2: 111.
- Ledru, M. P. 1993. Late Quaternary environmental and climatic changes in central Brazil. Quat. Res. 39: 90–98.
- Lessa, E. P., Cook, J. A. and Patton, J. L. 2003. Genetic footprints of demographic expansion in North America, but not Amazonia, during the Late Quaternary. – Proc. Natl Acad. Sci. USA 100: 10331–10334.
- Lijtmaer, D. A., Kerr, K. C. R., Stoeckle, M. Y. and Tubaro, P. L. 2012. DNA barcoding birds: from field collection to data analysis. In: Kress, W. J. and Erickson, D. L., (eds), DNA barcodes: methods and protocols. Methods in molecular biology, Vol. 858. Springer, pp. 127–152.
- Lougheed, S. C., Freeland, J. R., Handford, P. and Boag, P. T. 2000.
 A molecular phylogeny of warbling-finches (*Poospiza*): paraphyly in a Neotropical Emberizid genus. Mol. Phylogenet. Evol. 17: 367–378.
- Lovette, I. J. 2005. Glacial cycles and the tempo of avian speciation. Trends Ecol. Evol. 20: 57–59.
- Maia, R. and White, T. E. 2018. Comparing colors using visual models. Behav. Ecol. 29: 649–659.
- Maia, R., Eliason, C. M., Bitton, P. P., Doucet, S. M. and Shawkey, M. D. 2013. pavo: an R package for the analysis, visualization and organization of spectral data. – Methods Ecol. Evol. 4: 906–913.
- Maldonado-Coelho, M., Blake, J. G., Silveira, L. F., Batalha-Filho,
 H. and Ricklefs, R. E. 2013. Rivers, refuges and population divergence of fire-eye antbirds (*Pyriglena*) in the Amazon Basin.
 J. Evol. Biol. 26: 1090–1107.
- Morton, E. S. 1975. Ecological sources of selection on avian sounds. Am. Nat. 109: 17–34.
- Naka, L. N. and Brumfield, R. T. 2018. The dual role of Amazonian rivers in the generation and maintenance of avian diversity. Sci. Adv. 4: eaar8575.
- Nores, M. 1992. Bird speciation in subtropical South America in relation to forest expansion and retraction. Auk 109: 346–357.
- Nwankwo, E. C., Pallari, C. T., Hadjioannou, L., Ioannou, A., Mulwa, R. K. and Kirschel, A. N. G. 2017. Rapid song divergence leads to discordance between genetic distance and phenotypic characters important in reproductive isolation. – Ecol. Evol. 8: 716–731.
- Oksanen, J., Blanchet, F. G., Kindt, R., Legendre, P., Minching, P. R., O'Hara, R. B. and Wagner, H. 2008. Vegan: community ecology package. http://cc.oulu.fi/~jarioksa/softhelp/vegan.html.
- Oliveira-Filho, A. T. and Ratter, J. A. 1995. A study of the origin of central Brazilian Forest by the analysis of plant species distribution patterns. Edinb. J. Bot. 52: 141–194.
- Olrog, C. 1963. Lista y distribucion de las aves argentinas. Opera Lilloana 9: 1–377.
- Orme, C. D. L., Davies, R. G., Burgess, M., Eigenbrod, F., Pickup, N., Olson, V. A., Webster, A. J., Ding, T. S., Rasmussen, P. C., Ridgely, R. S., Stattersfield, A. J., Bennett, P. M., Blackburn, T. M., Gaston, K. J. and Owens, I. P. F. 2005. Global hotspots of species richness are not congruent with endemism or threat. Nature 436: 1016–1019.
- Paulo, P. et al. 2023. Geographic drivers of genetic and plumage color diversity in the blue-crowned manakin. Evol. Biol. 50: 413–431.
- Peterson, B. K., Weber, J. N., Kay, E. H., Fisher, H. S. and Hoekstra, H. E. 2012. Double digest RADseq: an inexpensive method for de novo SNP discovery and genotyping in model and non-model species. PLoS One 7: e37135.

- Pritchard, J. K., Stephens, M. and Donnelly, P. 2000. Inference of population structure using multilocus genotype data. – Genetics 155: 945–959.
- Rambaut, A., Drummond, A. J., Xie, D., Baele, G. and Suchard, M. A. 2018. Tracer v1.7. http://beast.community/tracer.
- Ribas, C. C., Aleixo, A., Nogueira, A. C. R., Miyaki, C. Y. and Cracraft, J. 2012. A palaeobiogeographic model for biotic diversification within Amazonia over the past three million years. – Proc. R. Soc. B 279: 681–689.
- Ronquist, F., Teslenko, M., van der Mark, P., Ayres, D. L., Darling, A., Höhna, S., Larget, B., Liu, L., Suchard, M. A. and Huelsenbeck, J. P. 2012. MrBayes 3.2: efficient Bayesian phylogenetic inference and model choice across a large model space. Syst. Biol. 61: 539–542.
- Rull, V. 2011. Neotropical biodiversity: timing and potential drivers. Trends Ecol. Evol. 26: 508–513.
- Sedano, R. E. and Burns, K. J. 2010. Are the northern Andes a species pump for Neotropical birds? Phylogenetics and biogeography of a clade of Neotropical tanagers (Aves: Thraupini). – J. Biogeogr. 37: 325–343.
- Seddon, N. 2005. Ecological adaptation and species recognition drives vocal evolution in Neotropical suboscine birds. – Evolution 59: 200–215.
- Siddiqi, A., Cronin, T. W., Loew, E. R., Vorobyev, M. and Summers, K. 2004. Interspecific and intraspecific views of color signals in the strawberry poison frog *Dendrobates pumillo*. J. Exp. Biol. 207: 2471–2485.
- Silva, J. M. 1994. Can avian distribution patterns in northern Argentina be related to retraction caused by quaternary climatic changes? – Auk 111: 495–499.
- Silva, S. M. et al. 2019. A dynamic continental moisture gradient drove Amazonian bird diversification. – Sci. Adv. 5: eaat5752.
- Smith, B. T. and Klicka, J. 2010. The profound influence of the Late Pliocene Panamanian uplift on the exchange, diversification and distribution of New World birds. – Ecography 33: 333–342.
- Smith, B. T., McCormack, J. E., Cuervo, A. M., Hickerson, M. J.,
 Aleixo, A., Cadena, C. D., Pérez-Emán, J., Burney, C. W., Xie,
 X., Harvey, M. G., Faircloth, B. C., Glenn, T. C., Derryberry,
 E. P., Prejean, J., Fields, S. and Brumfield, R. T. 2014. The
 drivers of tropical speciation. Nature 515: 406–409.
- Stamatakis, A. 2014. RAxML version 8: a tool for phylogenetic analysis and post-analysis of large phylogenies. Bioinformatics 30: 1312–1313.
- Tabachnick, B. and Fidell, L. 2001, Using multivariate statistics. Harper Collins College Publishers.
- Thom, G., Xue, A. T., Sawakuchi, A. O., Ribas, C. C., Hickerson, M. J., Aleixo, A. and Miyaki, C. Y. 2020. Quaternary climate changes as speciation drivers in the Amazon floodplains. Sci. Adv. 6: eaax4718.
- Thrasher, D. J., Butcher, B. G., Campagna, L., Webster, M. S. and Lovette, I. J. 2018. Double-digest RAD sequencing outperforms microsatellite loci at assigning paternity and estimating relatedness: a proof of concept in a highly promiscuous bird. – Mol. Ecol. Resour. 18: 953–965.
- Touchton, J. M., Seddon, N. and Tobias, J. A. 2014. Captive rearing experiments confirm song development without learning in a tracheophone suboscine bird. PLoS One 9: e95746.
- Trujillo-Arias, N., Calderón, L., Santos, F. R., Miyaki, C. Y., Aleixo, A., Witt, C. C., Tubaro, P. L. and Cabanne, G. S. 2018. Forest corridors between the central Andes and the southern Atlantic Forest enabled dispersal and peripatric diversification without

- niche divergence in a passerine. Mol. Phylogenet. Evol. 128: 221–232.
- Trujillo-Arias, N., Dantas, G. P. M., Arbeláez-Cortés, E., Naoki, K., Gómez, M. I., Santos, F. R., Miyaki, C. Y., Aleixo, A., Tubaro, P. L. and Cabanne, G. S. 2017. The niche and phylogeography of a passerine reveal the history of biological diversification between the Andean and the Atlantic forests. Mol. Phylogenet. Evol. 112: 107–121.
- Trujillo-Arias, N., Rodríguez-Cajarville, M. J., Sari, E., Miyaki, C. Y., Santos, F. R., Witt, C. C., Barreira, A. S., Gómez, I., Naoki, K., Tubaro, P. L. and Cabanne, G. S. 2020. Evolution between forest macrorefugia is linked to discordance between genetic and morphological variation in Neotropical passerines. Mol. Phylogenet. Evol. 149: 106849.
- Tubaro, P. L. and Lijtmaer, D. A. 2006. Environmental correlates of song structure in forest grosbeaks and saltators. – Condor 108: 120–129.
- Valderrama, E., Pérez-Emán, J. L., Brumfield, R. T., Cuervo, A. M. and Cadena, C. D. 2014. The influence of the complex topography and dynamic history of the montane Neotropics on the evolutionary differentiation of a cloud forest bird (*Premnoplex brunnescens*, Furnariidae). J. Biogeogr. 41: 1533–1546.
- van Els, P., Zarza, E., Rocha Moreira, L., Gómez-Bahamón, V., Santana, A., Aleixo, A., Ribas, C. C., Sena do Rêgo, P., Pérsio Dantas Santos, M., Zyskowski, K., Prum, R. O. and Berv, J. 2021. Recent divergence and lack of shared phylogeographic history characterize the diversification of Neotropical savanna birds. J. Biogeogr. 48: 1–10.
- Vorobyev, M. and Osorio, D. 1998. Receptor noise as a determinant of colour thresholds. Proc. R. Soc. B 265: 351–358.
- Vorobyev, M., Osorio, D., Bennett, A. T. D., Marshall, N. J. and Cuthill, I. C. 1998. Tetrachromacy, oil droplets and bird plumage colors. J. Comp. Physiol. A 183: 621–633.
- Wang, J. L. 2004. Application of the one-migrant-per-generation rule to conservation and management. Conserv. Biol. 18: 332–343.
- Weir, J. T. 2006. Divergent timing and patterns of species accumulation in lowland and highland Neotropical birds. Evolution 60: 842–855.
- Weir, J. T. 2009. Implications of genetic differentiation in Neotropical montane forest birds. – Ann. Miss. Bot. Gard. 96: 410–433.
- Weir, J. T. and Price, M. 2011. Andean uplift promotes lowland speciation through vicariance and dispersal in *Dendrocincla* woodcreepers. Mol. Ecol. 20: 4550–4563.
- Weir, J. T. and Schluter, D. 2004. Ice sheets promote speciation in boreal birds. Proc. R. Soc. B 271: 1881–1887.
- Weir, J. T. and Schluter, D. 2008. Calibrating the avian molecular clock. Mol. Ecol. 17: 2321–2328.
- Weir, J. T., Bermingham, E. and Schluter, D. 2009. The Great American Biotic Interchange in birds. – Proc. Natl Acad. Sci. USA 106: 21737–21742.
- Wiley, R. H. 1991. Associations of song properties with habitat for territorial oscine birds of eastern North America. – Am. Nat. 138: 973–993.
- Zheng, X., Levine, D., Shen, J., Gogarten, S. M., Laurie, C. and Weir, B. S. 2012. A high-performance computing toolset for relatedness and principal component analysis of SNP data. Bioinformatics 28: 3326–3328.
- Zurita, A., Boilini, R., Francia, A., Erra, G. and Alcaraz, M. 2014.
 Paleontología y cronología del Cuaternario de las provincias de Corrientes y Formosa, Argentina. Acta Geol. Lilloana 26: 75–86.